Pressure-Induced Phase Transition of Poly(oxymethylene) from the Trigonal to the Orthorhombic Phase: Effect of Morphological Structure

Masamichi Kobayashi* and Hirofumi Morishita†

Department of Macromolecular Science, Faculty of Science, Osaka University, Toyonaka, Osaka 560, Japan

Masaki Shimomura

Research Institute for Polymers and Textiles, Tsukuba, Ibaraki 305, Japan.
Received December 27, 1988

ABSTRACT: Pressure-induced solid-state phase transition of poly(oxymethylene) from the trigonal (t-POM) to the orthorhombic (o-POM) phase was investigated by means of infrared and Raman spectroscopies. Two t-POM samples different in crystal morphology, i.e., needlelike single crystals having a fully extended chain structure (ECC sample) and solution-grown lamellar crystals having a folded chain structure (FCC sample), were used as the starting materials. The orthorhombic phases generated from the ECC and FCC starting samples give rise to infrared spectra significantly different from each other; that is, the B_1 bands with transition moment parallel to the chain axis are remarkably shifted to the high-frequency side (by 92 cm^{-1} at the maximum) in the case generated from the FCC sample compared with those generated from the ECC sample. On the contrary, the B_2 and B_3 infrared bands with transition moments perpendicular to the chain axis as well as the A Raman bands appear at the same frequencies in the two cases. This very specific spectral feature in relation to crystal morphology is the same as for the case of t-POM where the A_2 infrared bands with parallel polarization exhibit selective large high-frequency shifts in the FCC sample compared with the ECC and highly oriented film samples. It was concluded that (1) the morphology of the starting t-POM sample was kept unaltered on the pressure-induced phase transition to o-POM and (2) the specific spectral change with change in crystal morphology found first in t-POM was the case also in o-POM. The origin of this phenomenon was considered.

Introduction

Poly(oxymethylene), $(CH_2O)_n$ (abbreviated as POM), crystallizes into two modifications: the stable trigonal form (t-POM) and the metastable orthorhombic form (o-POM). The trigonal form consists of the (9/5)[1] or (29/16)[2] helical molecules and is obtained exclusively through the ordinary crystallization processes from the melt or from solution. The orthorhombic form was prepared first by Mortillario et al.[3] through a polymerization of formaldehyde in aqueous solution, and its crystallographic unit cell consisting of two (2/1) helical molecules was determined by Carrazzolo and Mammi.[4] Thereafter, we have shown that this modification is obtained as a byproduct of a heterogeneous cationic polymerization of trioxane designed for preparing needlelike single crystals of t-POM.[5,6] In this process, o-POM appears in a plate-shaped single crystal with dimensions of 30–100-μm width and several microns thickness. With the plate-shaped single crystal, we investigated the thermal phase transition from o-POM to t-POM by means of the DSC and polarized Raman microprobe techniques[7] and revealed that the morphology as well as the molecular orientation was kept unaltered throughout the transition. As for another solid-state phase transition of POM, Miyaji and Asai[8] found by an X-ray diffraction study that t-POM transformed partly to o-POM by compressing a t-POM sample in a diamond anvil cell at a pressure as high as 14 kbar (1.4 GPa).

The trigonal form of POM is obtainable in various morphological structures between two extreme cases of the fully extended chain crystal (ECC) and the folded chain crystal (FCC), depending on the conditions of sample preparation and/or of sample processing. A typical ECC sample is obtained through a heterogeneous cationic polymerization of trioxane,[9,10] giving micron-sized needlelike single crystals (polymer whiskers) where the POM molecules align parallel to the needle axis. A typical FCC sample is obtained by crystallization from dilute solutions, say bromobenzene solution, giving hexagon-shaped lamellar crystals with thickness of about 100 μm.

In a series of previous papers,[11-14] we have demonstrated that the vibrational spectrum of t-POM exhibits a very specific change depending on the morphology of the sample. The bands due to the A_2 symmetry species, having the transition dipole along the chain axis, show very remarkable high-frequency shifts (by as large as 100 cm^{-1}) in the FCC sample compared with those of the ECC sample. On the other hand, the infrared- and Raman-active E_1 band (having the transition dipole perpendicular to the chain axis) and the Raman-active A_1 and E_2 bands appear at the same frequencies in both FCC and ECC samples. Such a very specific spectral feature can be used for the characterization of the morphological structure of t-POM samples.

In the present work, the pressure-induced phase transition from t-POM to o-POM is investigated by means of infrared and Raman spectroscopies, using typical ECC and FCC samples of t-POM as the starting materials. Our efforts are focused on solving the following problems. First, we are concerned with the role of the morphological structure in the solid-state transition. It is very important to know how the transition behavior is influenced by the morphology of the starting sample and whether the original morphology is retained or altered during the transition. Second, concerning the origin of the above-mentioned specific spectral feature found in t-POM, it is important to confirm whether the spectral change with morphology is limited to the case of t-POM or whether it is a generally observable phenomenon for a group of materials including o-POM. To this end, we try to clarify how the infrared and Raman spectra of o-POM generated through the pressure-induced transition are influenced by the morphology of the starting t-POM samples.

Experimental Section

The FCC sample of t-POM was deposited from a 0.5 wt % bromobenzene solution of Delrin 500 (E. I. du Pont de Nemours & Company, Inc., Wilmington, DE) kept at 130 °C. The precipitates were freeze-dried with *n*-hexane, giving a fine powder

† Present address: Faculty of Education, Nagasaki University, Nagasaki-City, Nagasaki 852, Japan.

0024-9297/89/2222-3726$01.50/0

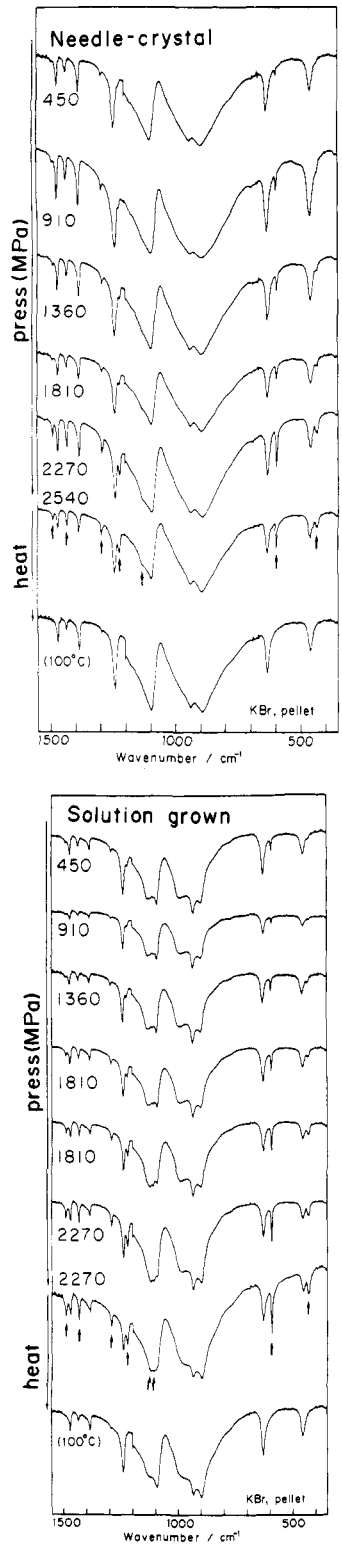

Figure 1. Infrared spectral changes in the mid-infrared region on the pressure-induced phase transition of poly(oxymethylene) from the trigonal to the orthorhombic phase and successive thermal transition in the reverse direction. The bands indicated by the arrows are due to the orthorhombic phase generated. Starting (top) from the needlelike single crystals (ECC sample) and (bottom) from the solution-grown lamellar crystals (FCC sample) of the trigonal phase.

sample. The ECC sample used was the needlelike single crystals prepared by a heterogeneous cationic polymerization of trioxane (using BF_3 catalyst).

The t-POM samples of both ECC and FCC, in the neat or in a mixture with KBr powder, were pressed in a piston cylinder cell made of stainless steel at a pressure up to 2.5 GPa for 10–30 min. After removal of pressure, the pellets obtained were picked

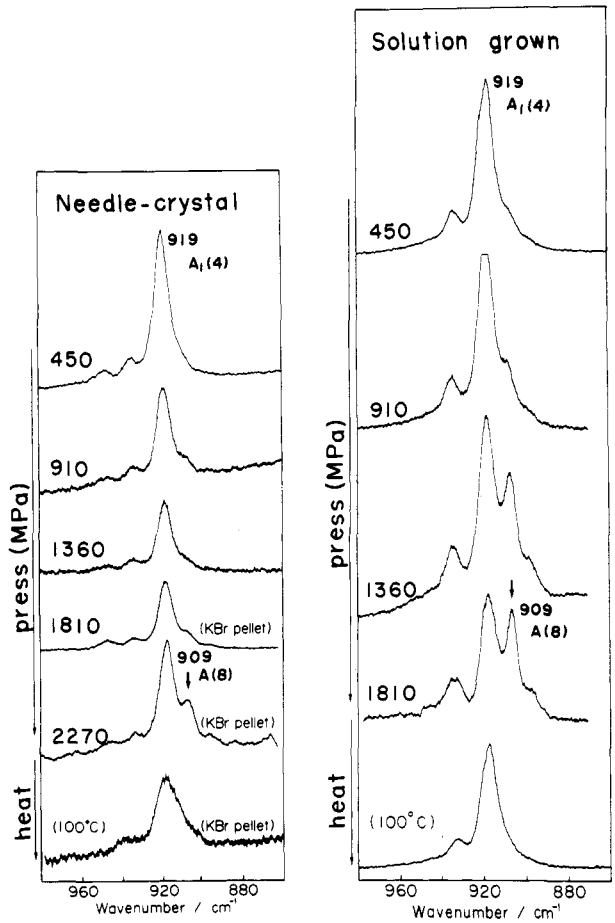

Figure 2. Raman spectral changes (in the C–O stretch region) on the pressure-induced phase transition of poly(oxymethylene) from the trigonal to the orthorhombic phase and successive thermal transition in the reverse direction. The band indicated by the arrow is due to the orthorhombic phase generated. Starting from the ECC (left) and FCC (right) samples of the trigonal phase.

out of the cell and subjected to the spectral measurements.

The absorption spectra in the mid-infrared region were measured with a JASCO A3 grating spectrometer and a JASCO 5MP FT-IR spectrometer. The far-infrared spectra were taken with a Hitachi FIS-3 grating spectrometer. The Raman spectra were measured with a JASCO R1000 double monochromator using the 514.5-nm excitation beam from an Ar^+ laser.

Results and Discussion

(1) Spectral Changes on Phase Transition. Changes in the mid-infrared spectrum of the ECC and FCC samples of t-POM with increasing magnitude of the applied pressure are shown in Figure 1. Of the two spectra indicated by the same magnitude of pressure, the lower one is of the sample compressed for a longer time. The absorption bands associated with the generated orthorhombic form (marked with the arrows) increase in intensity with increasing pressure or duration of compression. When the compressed sample is heated at 100 °C, all of the o-POM bands disappear completely through the thermal phase transition to t-POM, as indicated at the bottom of each spectrum.[7] The Raman spectral changes for the same procedures are reproduced in Figure 2.

The conversion of the pressure-induced phase transition is plotted as a function of the magnitude of applied pressure in Figure 3. Here, the conversion, c, was estimated from the absorption intensity ratio of the 630-cm^{-1} (t-POM) and 595-cm^{-1} (o-POM) infrared bands, I_{630}/I_{595}, according to the equation

$$1/c = 1 + [I_{630}/I_{595}][\epsilon_{595}/\epsilon_{630}]$$

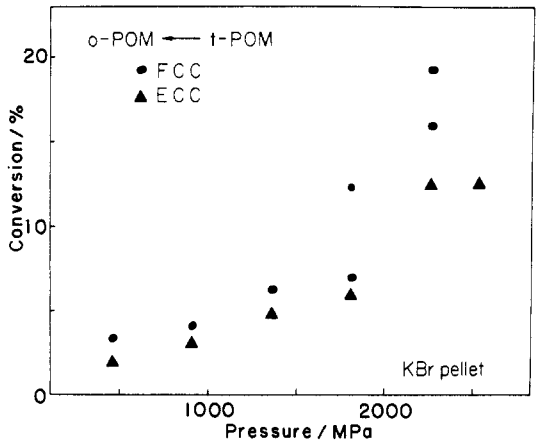

Figure 3. Pressure dependence of conversion to the orthorhombic phase from the ECC and FCC samples of poly(oxymethylene).

Table I
Symmetry Species, Number of Normal Modes, and Infrared and Raman Polarizations of Orthorhombic Poly(oxymethylene) (Space Group: $P2_12_12_1$-D_2^4)

species	internal modes	lattice modes	polarization	
			infrared	Raman
A	10	2 (R_c', T_c')	forbidden	α_{aa}, α_{bb}, α_{cc}
B_1	10	1 (R_c')	μ_c	α_{ab}
B_2	10	1 (T_a')	μ_b	α_{ac}
B_3	10	1 (T_b')	μ_a	α_{bc}

where the molar absorption coefficient ratio of the two bands, $\epsilon_{595}/\epsilon_{630}$, was evaluated as follows. The I_{595} and I_{630} values of a compressed sample were measured first, and the sample was heated at 100 °C to transform the orthorhombic phase to the trigonal phase, and then the increment in the I_{630} value on the thermal phase transition, ΔI_{630}, was measured. The ratio $\epsilon_{595}/\epsilon_{630} = I_{595}/\Delta I_{630}$ was obtained. Figure 3 indicates that the solution-grown FCC sample is more easily transformed to o-POM than the needlelike ECC sample.

It should be noted that the pressure-induced phase transition does not occur under the pure hydrostatic compression up to about 2 GPa as has been pointed out by Miyaji.[15] Therefore, some of the shear components of the stress tensor may contribute to the occurrence of the phase transition.

(2) Infrared Spectral Feature of the Generated Orthorhombic Phase. The unit cell of o-POM contains two (2/1) helical molecules, and the molecular vibrations of this modification are classified into four symmetry species, A, B_1, B_2, and B_3. The number of normal modes and the infrared and Raman polarizations are given in Table I. The B_1 modes are active in both infrared and Raman spectra, having the transition dipole parallel to the chain axis (the *c* axis). The B_2–B_3 pairs correspond to the Davydov split pairs due to the intermolecular interactions between two molecules in the unit cell. They have the transition dipole perpendicular to the chain axis.

Figure 4 shows the infrared spectral changes for the 10th B_2–B_3 split pair of o-POM, which corresponds to the 10th E_1 mode of t-POM, during the pressure-induced (t → o) transition and the successive thermal (o → t) transition measured on the FCC and ECC t-POM starting samples. In both cases, the B_2–B_3 split pair appears at the same frequencies. Figure 5 shows the far-infrared spectral changes during the same procedure for the 10th B_1 band of o-POM, which corresponds to the 5th A_2 band of t-POM. Contrary to the case of the B_2–B_3 pair, the $B_1(10)$ mode of o-POM generated from the solution-grown FCC t-POM sample appears at 316 cm^{-1}, while the same mode

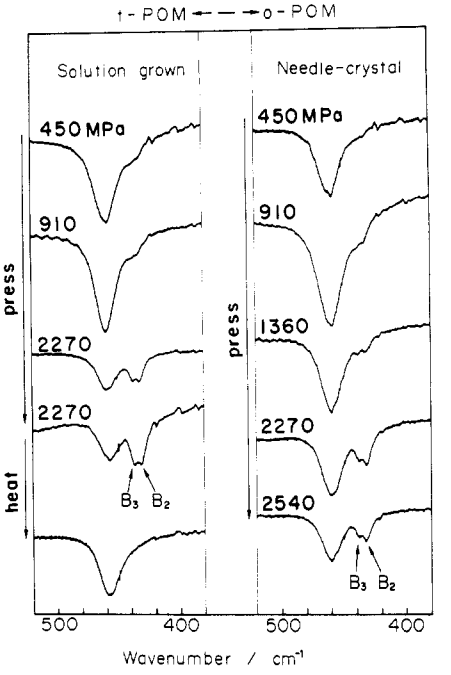

Figure 4. Infrared spectral changes of the 10th perpendicular fundamental [$E_1(10)$ of the trigonal phase and $B_2(10)$–$B_3(10)$ Davydov split pair of the orthorhombic phase] of poly(oxymethylene) on the pressure-induced phase transition from the trigonal to the orthorhombic phase. Starting from the FCC (left) and ECC (right) samples of the trigonal phase.

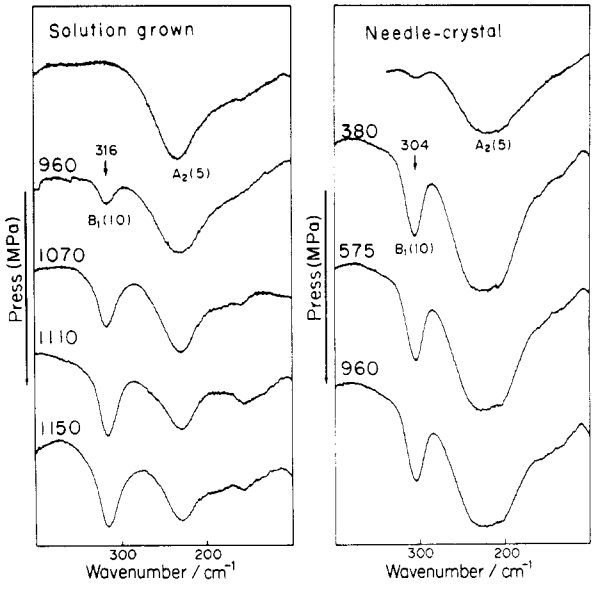

Figure 5. Far-infrared spectral changes of the torsional mode [$A_2(5)$ of the trigonal phase and $B_1(10)$ of the orthorhombic phase] on the pressure-induced phase transition of poly(oxymethylene) from the trigonal to the orthorhombic phase, starting from the FCC (left) and ECC (right) samples of the trigonal phase.

of o-POM generated from the needlelike ECC t-POM sample appears at 304 cm^{-1}. The latter frequency is very close to that of the plate-shaped single crystal (typical of ECC) of o-POM (at 297 cm^{-1}, Figure 6).[12] The discrepancy between 297 and 304 cm^{-1} may be caused by a little distortion of the perfect ECC structure during the compression. Therefore, 316 cm^{-1} of the o-POM generated from the FCC starting sample can be recognized as the $B_1(10)$ mode frequency of the FCC sample of o-POM. This is the same tendency as the case of t-POM, where the $A_2(5)$ mode appears at 236 cm^{-1} in the FCC sample, while it appears at 220 cm^{-1} in the ECC sample.[13]

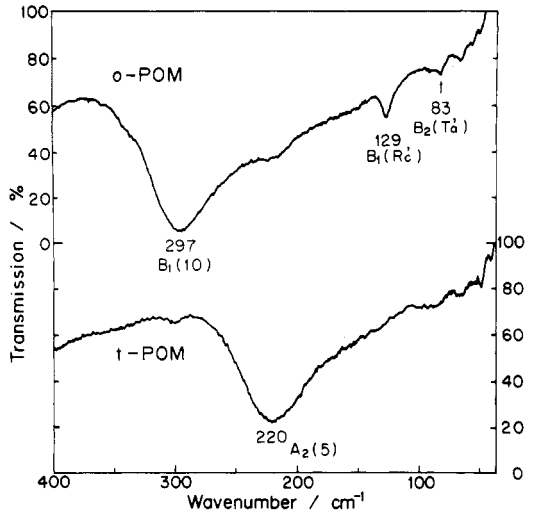

Figure 6. Far-infrared spectra of orthorhombic poly(oxymethylene) measured on an ECC sample prepared by a heterogeneous cationic polymerization of trioxane (upper) and of trigonal poly(oxymethylene) transformed from the ECC sample by the thermal transition (lower).

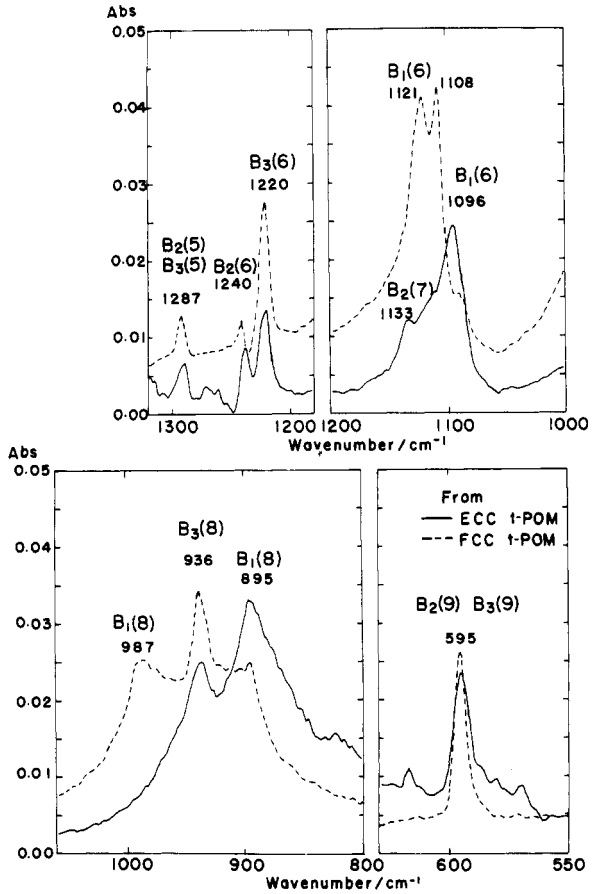

Figure 7. Fourier transform infrared spectra of pure orthorhombic poly(oxymethylene) generated by the pressure-induced phase transition from the ECC (—) and FCC (---) samples of the trigonal phase. The spectra are obtained by the subtraction technique (cf. text).

For other absorption bands in the mid-infrared region, the similar comparison was performed by using the subtraction technique in order to remove the interference by strong absorptions associated with the remaining t-POM. The infrared spectrum corresponding to pure o-POM generated from a particular starting t-POM sample was obtained by the following procedure. The spectrum of a compressed sample was recorded and memorized first

Table II
Frequencies of Infrared-Active Modes of ECC and FCC Samples of Trigonal and Orthorhombic Poly(oxymethylene) (cm^{-1})

(a) Trigonal Poly(oxymethylene)

mode	drawn film	ECC[a]	FCC[b]	$\Delta\nu$[c]
$E_1(3)$	1471 (⊥) m	1470	1470	0
$E_1(4)$	1434 (⊥) w	1433	1434	1
$A_2(2)$	1381 (∥) m	1385	1385	0
$E_1(5)$	1286 (⊥) vw	1291	1291	0
$E_1(6)$	1235 (⊥) vs	1235	1235	0
$A_2(3)$	1097 (∥) vvs	1097	1136	39
$E_1(7)$	1091 (⊥) vvs	*f*	1092	
$E_1(8)$	932 (⊥) vvs	935	935	0
$A_2(4)$	903 (∥) vvs	897	1002	105
$E_1(9)$	630 (⊥) s	628	630	2
$A_2(5)$	230 (∥) m	220	236	16

(b) Orthorhombic Poly(oxymethylene)

mode	ECC[d]	FCC[e]	$\Delta\nu$[c]
$B_2(5)+B_3(5)$	1287 m	1287 m	0
$B_2(6)$	1240 m	1240 m	0
$B_3(6)$	1220 s	1220 s	0
$B_2(7)$	1133 s	*g*	
$B_3(7)$	*g*	1108 vvs	
$B_1(6)$	1096 vvs	1121 vvs	25
$B_1(8)$	895 vvs	987 vvs	92
$B_3(8)$	936 vvs	936 vvs	0
$B_2(9) + B_3(9)$	595 vs	595 vs	0
$B_3(10)$	434 m	434 m	0
$B_2(10)$	428 m	428 m	0
$B_1(10)$	304 m	316 m	12

[a] Needlelike single crystals obtained by a cationic polymerization of trioxane. [b] Solution-grown lamellar crystals deposited from a bromobenzene solution. [c] Frequency gap: ν(FCC) − ν(ECC). [d] Rod-like single crystals obtained as a byproduct of a cationic polymerization of trioxane. [e] Obtained from the FCC sample of trigonal poly(oxymethylene) through pressure-induced phase transition. [f] Interferred by a strong A_2 band. [g] Interferred by a strong B_1 band.

(spectrum A); then the sample was heated at 100 °C in order to convert the generated orthorhombic phase to the trigonal phase, and its spectrum was recorded (spectrum B). The subtraction spectrum A–B gave the spectrum corresponding to the pure o-POM generated by the pressure-induced transition. The obtained spectra of o-POM generated from the ECC and FCC t-POM samples are compared with each other in Figure 7. The $B_1(6)$ and $B_1(8)$ modes exhibit a very remarkable high-frequency shift in the spectrum generated from the FCC sample, whereas the B_2 and B_3 modes appear at the same frequencies in both samples.

The frequencies of the infrared-active modes of t-POM and o-POM measured on two samples of different sources are summarized in Table II. In both modifications, very specific frequency shifts caused by the difference in morphological structure are observed for the infrared-active vibrational modes, having the transition dipole parallel to the chain axis, i.e., the A_2 modes of t-POM and the B_1 modes of o-POM. The Raman-active A modes appear at the same frequencies in ECC and FCC samples (see Figure 2).

From these experimental results, we are able to deduce the following conclusions: (1) the ECC or FCC structure of the starting t-POM is retained in the pressure-induced phase transition, and (2) the very specific infrared spectral change accompanied with the change in the chain-folding structure found first in t-POM is observed also in o-POM.

It has been believed that vibrational spectra in the mid-infrared region are insensitive to the difference in such a higher order structure as crystal morphology. Never-

Table III
Frequency Gaps of A_2 Modes of Trigonal Poly(oxymethylene) between FCC and ECC Samples and Absorption Intensities

mode	ν(ECC), cm^{-1}	ν(FCC), cm^{-1}	$\Delta\nu$, cm^{-1}	A^a	A/ν(ECC)^b
$A_2(1)$	2985	2985	~0		
$A_2(2)$	1385	1385	~0	1	1
$A_2(3)$	1097	1136	39	20	25
$A_2(4)$	897	1002	105	60	93
$A_2(5)$	220	236	16	2	13

[a] Relative integrated intensity reduced to the value of the $A_2(2)$ mode. [b] Relative oscillator strength reduced to the value of the $A_2(2)$ mode.

theless, the present result suggests that the large frequency shift for some specific vibrational modes caused by the morphological change is not limited to POM but is possibly a generally observable phenomenon for a group of polymers. Since POM is characterized by its exceptionally strong infrared absorption compared with other organic compounds, we supposed that the specific spectral feature we found was related to the large transition moment of POM. With this prediction, we searched other polymers that exhibited the same trend and found that poly(ethylene oxide) showed a similar but less significant (the maximum magnitude of the frequency shift was 19 cm^{-1}) spectral difference between the well-drawn films (ECC) and the solution-grown lamellar crystals (FCC).[17]

The origin of this phenomenon is not fully clarified. However, the magnitude of the frequency shift is related to the infrared intensity and the normal frequency. In Table III, the relative integrated intensities, A, and the oscillator strengths, A/ν (ν is the normal frequency), of the A_2 modes of t-POM (reduced to those of the $A_2(2)$ mode) are compared with the frequency gaps, $\Delta\nu$, between the FCC and ECC samples. It is evident that $\Delta\nu$ is approximately proportional to A/ν. Therefore, this phenomenon may be caused by strong transition–dipole interactions, as the theory of frequency shift caused by the phase change from gaseous to solid state (Davydov splitting) predicts.[18,19] In that case, the magnitude of the Davydov splitting of the polar molecular system is proportional to $(\partial\mu/\partial Q)^2/\nu$ (Q is the normal coordinate). In our recent work on t-POM oligomers, we obtained the evidence that indicated that the high-frequency shift in the FCC sample is caused not by the folding structure itself but by its short stem length.[20] The short stem length disturbs the infrared selection rule for the infinitely long chain and gives infrared activity for some parallel modes in the vicinity of the zone center. These infrared-active modes produce additional high-frequency shift by the transition–dipole interaction. The effect of the conformational distortion by the chain folding does not play an important role, because if it were the case the frequencies of all the symmetry species should be influenced. We are currently working to make a more complete and quantitative interpretation of this very characteristic spectral feature from a theoretical point of view.

Acknowledgment. This work was supported by a Grant-in-Aid for Scientific Research on Priority Areas, New Functional Materials—Design, Preparation and Control, The Ministry of Education, Science and Culture (No. 63604014).

Registry No. POM, 9002-81-7.

References and Notes

(1) Tadokoro, H.; Yasumoto, T.; Murahashi, S.; Nitta, I. *J. Polym. Sci.* **1960**, *44*, 266. Uchida, T.; Tadokoro, H. *J. Polym. Sci., Polym. Phys. Ed.* **1967**, *5*, 63.
(2) Carazzolo, G. A. *J. Polym. Sci., Part A* **1963**, *1*, 1573.
(3) Mortillario, L.; Galliazzo, G.; Bessi, S. *Chem. Ind. (Milan)* **1964**, *46*, 139, 144.
(4) Carazzolo, G. A.; Mammi, M. *J. Polym. Sci., Part A* **1963**, *1*, 965.
(5) Kobayashi, M.; Itoh, Y.; Tadokoro, H.; Shimomura, M.; Iguchi, M. *Polym. Commun.* **1983**, *24*, 38.
(6) Iguchi, M. *Polymer* **1983**, *24*, 915.
(7) Kobayashi, M.; Morishita, H.; Shimomura, M.; Iguchi, M. *Macromolecules* **1987**, *20*, 2453.
(8) Miyaji, H.; Asai, K. *J. Phys. Soc. Jpn.* **1974**, *36*, 1497.
(9) Iguchi, M. *Br. Polym. J.* **1973**, *5*, 195.
(10) Iguchi, M.; Murase, I.; Watanabe, K. *Br. Polym. J.* **1974**, *6*, 61.
(11) Shimomura, M.; Iguchi, M. *Polymer* **1982**, *23*, 509.
(12) Kobayashi, M.; Morishita, H.; Ishioka, T.; Iguchi, M.; Shimomura, M.; Ikeda, T. *J. Mol. Struct.* **1986**, *146*, 155.
(13) Shimomura, M.; Iguchi, M.; Kobayashi, M. *Polymer* **1987**, *29*, 351.
(14) Morishita, H.; Kobayashi, M.; Komatsu, T. *Rep. Prog. Polym. Phys. Jpn.* **1987**, *30*, 127.
(15) Miyaji, H. *J. Phys. Soc. Jpn.* **1975**, *39*, 1346.
(16) Morishita, H.; Kobayashi, M. *Rep. Prog. Polym. Phys. Jpn.* **1987**, *30*, 131.
(17) Shimomura, M.; Tanabe, Y.; Watanabe, Y.; Kobayashi, M., submitted for publication in *Polymer*.
(18) Hexter, R. M. *J. Chem. Phys.* **1960**, *33*, 1833; **1962**, *36*, 2285.
(19) Yamada, H.; Person, W. B. *J. Chem. Phys.* **1964**, *40*, 309.
(20) Shimomura, M.; Iguchi, M.; Kobayashi, M., submitted for publication in *Polymer*.